

A comparison of electrophysiological properties of the CNGA1, CNGA1_{tandem} and CNGA1_{cys-free} Channels

Monica Mazzolini · Anil V. Nair · Vincent Torre

Received: 5 February 2008 / Accepted: 10 March 2008 / Published online: 1 April 2008
© EBSA 2008

Abstract Three constructs are used for the analysis of biophysical properties of CNGA1 channels: the WT CNGA1 channel, a CNGA1 channel where all endogenous cysteines were removed (CNGA1_{cys-free}) and a construct composed of two CNGA1 subunits connected by a small linker (CNGA1_{tandem}). So far, it has been assumed, but not proven, that the molecular structure of these ionic channels is almost identical. The I/V relations, ionic selectivity to alkali monovalent cations, blockage by tetracaine and TMA⁺ were not significantly different. The cGMP dose response and blockage by TEA⁺ and Cd²⁺ were instead significantly different in CNGA1 and CNGA1_{cys-free} channels, but not in CNGA1 and CNGA1_{tandem} channels. Cd²⁺ blocked irreversibly the mutant channel A406C in the absence of cGMP. By contrast, Cd²⁺ did not block the mutant channel A406C in the CNGA1_{cys-free} background (A406C_{cys-free}), but an irreversible and almost complete blockage was observed in the presence of the cross-linker M-4-M. Results obtained with different MTS cross-linkers and reagents suggest that the 3D structure of the CNGA1_{cys-free} differs from that of the CNGA1 channel and that the distance between homologous residues at position 406 in CNGA1_{cys-free} is longer than in the WT CNGA1 by several Angstroms.

Abbreviations

CNG Cyclic nucleotide-gated
CNBD Cyclic nucleotide-binding domain

CSM	Cysteine scanning mutagenesis
MTS	Methanethiosulfonate
MTSET	2-(Trimethylammonium)ethyl] methanethiosulfonate bromide
MTSPT	3-(Trimethylammonium)propyl methanethiosulfonate bromide
MTS-PtrEA	3-(Triethylammonium)propyl methanthiosulfonate bromide
M-2-M	1,2-Ethanediy] bismethanethiosulfonate
M-4-M	1,4-Butanediy] bismethanethiosulfonate
M-6-M	1,6-Hexanediy] bismethanethiosulfonate
M-8-M	3,6-Dioxaoctane-1,8-diyl bismethanethiosulfonate
M-11-M	3,6,9-Trioxaundecane-1,11-diyl bismethanethiosulfonate

Introduction

Cyclic nucleotide gated (CNG) channels mediate sensory transduction in photoreceptors and olfactory sensory neurons (Fesenko et al. 1985). In these cells, sensory transduction requires the binding of cyclic nucleotides (cGMP for photoreceptor and cAMP for olfactory receptor) to CNG channels in order for the latter to open (Craven and Zagotta 2006; Kaupp et al. 1989; Kaupp and Seifert 2002; Matulef and Zagotta 2003; Zagotta and Siegelbaum 1996). Native CNG channels are heterotetramers and have distinct subunits usually referred to as CNGA and CNGB (Bradley et al. 2001). Native CNG channels from bovine rod photoreceptors are composed of three CNGA1 and one CNGB1 subunits (Weitz et al. 2002; Zheng et al. 2002; Zhong et al. 2002). The CNGA1 subunit from bovine rod is composed of 690 amino acids

M. Mazzolini · A. V. Nair · V. Torre (✉)
International School for Advanced Studies,
via Beirut 2-4, 34014 Trieste, Italy
e-mail: torre@sissa.it

encoding for a cyclic nucleotide-binding (CNB) domain composed of about 125 amino acids in the cytoplasmic C-terminal end (Biel et al. 1999; Zagotta and Siegelbaum 1996). The analysis of the amino acid sequence of the CNGA1 subunit indicates the existence of six transmembrane segments, usually referred to as S1, S2, S3, S4, S5 and S6 helices. Between the S5 and S6 helices there is a pore region, from Val348 to Pro367, that shows a significant sequence homology with the pore region of K⁺ channels (Becchetti et al. 1999; Liu and Siegelbaum 2000). The overall architecture places CNG channels in the superfamily of voltage-gated ionic channels, rather than in the superfamily of ligand gated channels (Jan and Jan 1990). Homotetrameric CNGA1 channels from bovine rods, when heterologously expressed in *Xenopus leavis* oocytes, give rise to functional channels with properties similar—but not identical—to those of native CNG channels (Kaupp et al. 1989).

In order to understand the relation between structure and function of ionic channels, residues were mutated and electrophysiological properties of mutant channels were investigated. A common strategy is to substitute native residues with exogenous cysteines and to analyze the effect of compounds known to react with the sulfur (S) atom of cysteines. This procedure usually known as cysteine scanning mutagenesis (CSM) (Akabas et al. 1992; Karlin and Akabas 1998) analyses the formation of S–S bridges, spontaneously occurring or induced by appropriate cross-linking reagents, such as copper phenanthroline, Cd²⁺ ions or MTS–MTS compounds (Glusker 1991; Hastrup et al. 2001; Loo and Clarke 2001; Ren et al. 2006). As native ionic channels have endogenous cysteines, it is not easy to distinguish between the formation of S–S bridges between a pair of exogenous cysteines and between exogenous and endogenous cysteines. This issue is particularly relevant in studies aiming at establishing distances between homologous residues. Matulef et al. (1999) have engineered a CNGA1 channel (CNGA1_{cys-free}) where all endogenous cysteines were replaced with other residues not bearing an S atom. When exogenous cysteines are introduced in the CNGA1_{cys-free} any effect mediated by agents reacting with thiol groups can be ascribed to exogenous cysteines.

Another very useful construct is the CNGA1_{tandem} where two CNGA1 subunits are joined together by a small linker composed of some tens of residues (Flynn and Zagotta 2003; Matulef and Zagotta 2002; Rosenbaum and Gordon 2002; Rothberg et al. 2002). By introducing a mutation in only one subunit of the tandem it is possible to study the effect caused by the mutations in only two subunits out of the four composing the channel. In this way, a mutation that does not lead to functional channels when performed in all four subunits, may lead to functional channels when

performed in only two subunits. This enabled an extensive CSM in the pore region of CNGA1 channels (Liu and Siegelbaum 2000) extending the analysis to mutant channels otherwise not functional (Becchetti and Gamel 1999; Sun et al. 1996). All these constructs are very useful if the molecular structure of the CNGA1, CNGA1_{cys-free} and CNGA1_{tandem} is always the same or, if not, it is very similar.

In order to verify and to quantify these similarities, physiological properties of these channels were extensively compared by performing electrophysiological experiments where experimental variations were minimized. Ionic selectivity, cGMP dependency and blockage by a variety of compounds were investigated. Our results indicate that the electrophysiological properties of the CNGA1 and CNGA1_{tandem} are not significantly different. By contrast, differences between several electrophysiological properties of CNGA1 and CNGA1_{cys-free} are statistically significant. In addition, we show that Cd²⁺ ions in the absence of cGMP block irreversibly the mutant channels A406C and A406C&C481A&C505T in the WT background. By contrast, Cd²⁺ ions did not block the mutant channel A406C constructed in the CNGA1_{cys-free}, but an irreversible blockage was observed in the closed state by the application of the cross-linker M–4–M (Loo and Clarke 2001). Blockage of mutant channel A406C_{cys-free} was not observed in the presence of MTS derivatives with the same length and a volume larger than that of M–4–M able to link covalently to only one cysteine. These results indicate that homologous residues at position 406 in the CNGA1_{cys-free} are more distant by some Angstrom than in the CNGA1 channel. Functional differences between native and cysteine free proteins have already been reported and investigated (Kato et al. 1988; Kohler et al. 2003; Taylor et al. 2001), but their structural differences were rarely quantified. The present manuscript aims to quantify these differences.

Materials and methods

Molecular biology

Three different bovine rod channel constructs were used. The CNGA1 channel, consisting of 690 residues, the CNGA1_{tandem}, a tandem dimer construct and—a gift from William Zagotta—the CNGA1_{cys-free} channel (Matulef et al. 1999). Selected residues were replaced by introducing a cysteine in the CNGA1 and CNGA1_{cys-free} as previously described (Becchetti et al. 1999; Matulef et al. 1999) with the use of a Quick Change Site-Directed Mutagenesis kit (Stratagene). Point mutations were confirmed by sequencing them with the sequencer LI-COR 4200 series

(LI-COR, Lincoln, NE). cDNAs were linearized and was transcribed to cRNA in vitro using the mMessage mMachine kit (Ambion, Austin, TX).

The tandem dimer construct was generated by the insertion of one copy of the CNGA1 DNA into a vector pGEMHE already containing another copy of CNGA1 DNA. At the end of cloning two copies of the CNGA1 DNA, they were connected by a 10-amino acid linker GSGGTELGST (Rothberg et al. 2002) joining the C-terminus of the first CNGA1 with the N-terminus of the second one. This second subunit was made by replacing the *ApaI* restriction site “GGGCCC” at the end of the CNGA1 DNA without changing the amino acid “GGTCCC” and adding at the start codon a new *ApaI* restriction site followed by a linker, using a PCR reaction. Subunits were linked after *HindIII/ApaI* cut.

Oocyte preparation and chemicals

Mutant channel cRNAs were injected into *Xenopus laevis* oocytes (“Xenopus express” Ancienne Ecole de Vernassal, Le Bourg 43270, Vernassal, Haute-Loire, France). Oocytes were prepared as already described (Nizzari et al. 1993). Injected eggs were maintained at 18°C in a Barth solution supplemented with 50 µg/ml gentamycin sulfate and containing (in mM): 88 NaCl, 1 KCl, 0.82 MgSO₄, 0.33 Ca(NO₃)₂, 0.41 CaCl₂, 2.4 NaHCO₃, 5 TRIS–HCl, pH 7.4 (buffered with NaOH). During the experiments, oocytes were kept in a Ringer solution containing (in mM): 110 NaCl, 2.5 KCl, 1 CaCl₂, 1.6 MgCl₂, 10 HEPES–NaOH, pH 7.4 (buffered with NaOH). Usual salts and reagents were purchased from Sigma Chemicals (St Louis, MO, USA), and MTS compounds (MTSET, MTSPT, MTSPtrEA and cross-linkers) were purchased from TRC (Toronto Research Chemicals, Canada). MTSET, MTSPT, MTSPtrEA link covalently to only one cysteine. Cross-linker compounds such as M–2–M (1,2-Ethanediyl bismethanethiosulfonate), M–4–M (1,4-Butanediyl bismethanethiosulfonate), M–6–M (1,6-Hexanediyl bismethanethiosulfonate), M–8–M (3,6-Dioxaoctane-1,8-diyl bismethanethiosulfonate) and M–11–M (3,6,9-Trioxaundecane-1,11-diyl bismethanethiosulfonate) had different maximum cross-linking span—i.e., the longest distance between the S atoms of the cross-linker reacting with the S atoms of cysteine and forming S–S bonds (see Fig. 1) (Loo and Clarke 2001). These compounds, in contrast, can link to two cysteines.

The cross-linker M–2–M has a cross-linking span of 5.2 Å and an actual volume of 139 Å³. When M–2–M reacts with an S atom it loses one SO₂CH₃ group and when it cross-links with two S atoms its effective volume becomes 73.8 Å³. Longer cross-linkers, such as M–4–M, M–6–M, M–8–M and M–11–M can exist in different

configurations, i.e. they have several rotamers illustrated in the first column of Fig. 1.

The different effect of reagents able to link to one cysteine—such as MTSET, MTSPT, MTSPtrEA—and those able to link to two cysteines—M–X–M cross-linkers—with the same size and volume is used to discriminate whether blockage is caused by bridging two cysteines by the binding of the compound to one end only.

Recording apparatus














cGMP-gated currents from excised patches were recorded with a patch-clamp amplifier (Axopatch 200B, Axon Instruments Inc., Foster City, CA, USA), 2–6 days after RNA injection, at room temperature (20–24°C). The perfusion system was as described (Sesti et al. 1995) and allowed a complete solution change in less than 1 s. Borosilicate glass pipettes had resistances of 3–5 MΩ in symmetrical standard solution. The standard solution on both sides of the membrane consisted of (in mM) 110 NaCl, 10 HEPES and 0.2 EDTA (pH = 7.4). The membrane potential was usually stepped from 0 to ±100 mV in 20 mV steps or ±60 mV. We used Clampex 8.0, Clampfit, and Matlab for data acquisition and analysis. Currents were low-pass filtered at 2 kHz and acquired digitally at 5 kHz.

Application of sulfhydryl-specific reagents

In the inside-out patch-clamp configuration, soon after patch excision, the cytoplasmic face of the plasma membrane was perfused with the same pipette-filling solution and then by adding 1 mM cGMP to it. The effect of divalent cations was tested by perfusing the intracellular side of the membrane with a standard solution without EDTA (to avoid partial divalent cation chelation), supplemented with variable concentrations of CdCl₂ or 1 mM CaCl₂ for different periods of time to study their effect in the closed state. In order to study the open state effect we applied these solutions in the presence of 1 mM cGMP.

Cross-linker compounds were dissolved in dimethyl sulfoxide (DMSO) and diluted in standard solution to a final concentration of 100 µM. The final concentration of DMSO was 0.1%. We checked that this concentration of DMSO did not affect the cGMP activated current. Solutions containing cross-linker compounds were prepared immediately before the application (typically <5 min) to prevent degradation, as these reagents dissociate rapidly in aqueous solution. They were not used for more than 45 min after dissolving in aqueous solution. The cross-linkers of different length were used to determine the distance between exogenously introduced cysteines (Loo and Clarke 2001; Ren et al. 2006).

Fig. 1 Properties of different crosslinkers and the three channels under investigation. Properties of cross-linkers with handles of increasing length. The *first column* shows the chemical structure and some representative rotamers. The *spheres* shown in *yellow* represent sulfurs, oxygens are in *red*, carbons are in *grey* and hydrogens are in *white*. The suffixes *rot1* and *rot2* show two representative rotamers of a minimum and intermediate spacer arm length. The cross linking span of the M–X–M is calculated by the estimated chemical bond size (Loo and Clarke 2001) and the rotamers' cross-linking span was calculated by using the VMD visualization software (Humphrey et al. 1996) (*second column*). The actual volume is the volume with the SO_2CH_3 (shown as transparent objects) group at both ends (*third column*). The effective volume is the volume when the cross-linker loses its SO_2CH_3 groups to form bonds with the sulfur of cysteines (*fourth column*). The volumes are calculated using the program steric v1.12 (White et al. 1993)

	MTS cross-linkers	Maximum cross-linking span (Å)	Actual Volume (Å ³)	Effective Volume (Å ³)
	M-2-M	5.2	139.0	73.80
	M-4-M	7.8	166.4	101.2
	M-4-M _{rot1}	4.9	160.7	99.2
	M-4-M _{rot2}	6.5	174.2	102.5
	M-6-M	10.4	200.3	133.6
	M-6-M _{rot1}	5.7	193.9	132.8
	M-6-M _{rot2}	6.7	201.2	131.9
	M-8-O ₂ M	13	182.0	130.4
	M-8-O ₂ M _{rot1}	3.9	183.3	110.9
	M-8-O ₂ M _{rot2}	9.3	189.4	106.2
	M-11-O ₃ M	16.9	224.6	157.6
	M-11-O ₃ M _{rot1}	3.8	223.7	159.1
	M-11-O ₃ M _{rot2}	12.1	225.2	163.7

Comparison of electrophysiological properties

In order to reduce the sources of variability in the comparison of electrophysiological properties, several precautions were taken. Solutions from the same stock were used to fill the patch pipette or to perfuse the intracellular side of the membrane in all three channels. In all experiments the mRNA of the three channels were injected in oocytes harvested from the same animal. Each experiment was repeated at least three times in the same experimental session. Statistical significance of different properties between two channels was analyzed using Student's *t* test. For every data set, the current measured after a given chemical manipulation (Y_{iA} ($i = 1, n$)) was normalized ($A_i = Y_{iA}/X_{iA}$) to the current measured in control condition (X_{iA} ($i = 1, n$)). We used the Shapiro–Wilk test (Shapiro and Wilk 1965) to verify that normalized data had a Gaussian distribution. Variance comparison of normalized data were obtained by using the one sided *F* variance ratio method (Snedecor and Cochran 1989). Statistical significance was established using Student's *t* test. Statistical

difference was assumed to be high when $***P < 0.001$, medium when $**P < 0.01$ and marginal when $*P < 0.05$.

Results

The membrane topology of a single subunit of the CNGA1 channel from bovine rod is composed by six transmembrane segments, named S1, S2, S3, S4, S5, S6 containing seven native cysteines: Cys35, Cys169, Cys186, Cys314, Cys481, Cys505 and Cys573.

Cys35 is located near the N-terminal of the CNGA1 channel at the cytoplasmic side (Brown et al. 1998; Molday et al. 1991) and it is thought to interact with Cys481 in the open state, but not in the closed state (Gordon et al. 1997; Rosenbaum and Gordon 2002). Cys169 and Cys186 are located in S1 and their functional and/or structural role has not been studied in detail. Cys314 in the S5 transmembrane segment can interact with residues at position 380 in the S6 domain (Nair et al. 2006). Cys481 is located in the C-linker region (Brown et al. 1998) and its role in channel function

has been extensively studied. Modification of Cys481 in the open state with sulfhydryl reagents potentiates CNGA1 channels (Brown et al. 1998). Cys505 in the CNB domain is accessible to sulfhydryl reagents in the closed state but not in the open state (Matulef et al. 1999; Sun et al. 1996). Finally, Cys573 is located near the C-terminus of the channel. Cys573 does not contribute to the potentiation observed by the application of compounds promoting the formation of disulfide bonds (Gordon et al. 1997) and does not seem to have any structural and functional role. Therefore Cys481 and Cys505 are the native cysteines in the C-linker region and in the CNB domain.

In the CNGA1_{cys-free} the seven native cysteines were replaced by other aminoacids as described (Matulef et al. 1999). In CNGA1_{tandem} channels, the N-terminal of the CNGA1 channel is linked to the C-terminal of another copy of the CNGA1 channel by a few aminoacid linker (Flynn and Zagotta 2003; Gordon and Zagotta 1995; Liu and Siegelbaum 2000; Rosenbaum and Gordon 2002; Varum and Zagotta 1996).

In the following, an extensive comparison of physiological properties of the CNGA1, CNGA1_{tandem} and CNGA1_{cys-free} channels will be presented.

Electrophysiological differences among the three channels

cGMP activated currents from CNGA1 and CNGA1_{tandem} channels were recorded within one or two days after mRNA injection, but one or two additional days were necessary to obtain a comparable current from CNGA1_{cys-free} channels. As shown in Fig. 2a–c current recordings elicited in voltage clamp mode from membrane patches excised from oocytes injected with the mRNA of the three channels were very similar. In all three channels, when the voltage was stepped from 0 mV to ± 100 in 20 mV steps, the current reached its steady value within 2–4 ms. No time dependent relaxation of the cGMP activated current was observed. The I/V relations in the three channels under consideration were very similar but the dependency of the activated current on the cGMP concentration and blockage by Cd²⁺ ions and TEA⁺ was different in the CNGA1_{cys-free} and CNGA1 channels, as shown in Fig. 2.

The dose response, is shown in Fig. 2d for the CNGA1, CNGA1_{tandem} and CNGA1_{cys-free} channels. The cGMP concentration activating a half maximal current ($K_{1/2}$) was 116.9 ± 7.2 ($N = 7$ patches), 96.6 ± 7.7 ($N = 5$) and 27.5 ± 6.1 μM ($N = 6$) for the three channels, respectively. In agreement with Matulef et al. (1999), the CNGA1_{cys-free} channel has higher cGMP affinity than CNGA1 channel. The Student's *t* test indicated that the difference between the $K_{1/2}$ of CNGA1_{cys-free} and CNGA1 channels is highly significant ($***P < 0.0001$) and the

difference between the $K_{1/2}$ of CNGA1_{tandem} and CNGA1 channels is only marginal ($*P < 0.05$) (Fig. 2e).

Having compared the cGMP dose response we compared blockage by different compounds added at the intracellular side of the membrane. Blockage by divalent cations (Colamartino et al. 1991), TEA⁺, TMA⁺ (Menini 1990; Picco and Menini 1993) and tetracaine (Fodor et al. 1997a, b) was analyzed. These compounds have a different size and blocking mechanism and therefore their blockage can be used to probe the molecular environment of the intracellular side of the channel. TEA⁺ is a larger organic cation compared to TMA⁺ and its blocking effect on the current carried by Na⁺ ions in CNG channels is more effective (Menini 1990; Picco and Menini 1993). The WT CNGA1 channel does not have any cysteine residue in the pore region and therefore any effect of Cd²⁺ ions on the inner pore of CNGA1 channels cannot be ascribed to interactions with thiol groups. In all channels Cd²⁺ ions potentiated the amplitude of the cGMP activated current at negative voltages. However, at +100 mV we consistently observed a lower blockage in CNGA1_{cys-free} channels (see Fig. 2f). The different blockage at +100 mV observed in the CNGA1_{cys-free} was statistically significant (*t* test provides a value of $**P < 0.001$). The effect caused by the addition of Cd²⁺ ions were both quickly and entirely reversible as soon as Cd²⁺ ions were removed from the bathing medium.

The blockage of CNG channel by organic cations requires a concentration of the order of 10^{-2} M and therefore their blockage is less potent compared to Cd²⁺ requiring concentrations 10 and 100 times lower. We analyzed blockage by TMA⁺ and TEA⁺ when 110 mM Na⁺ was present on both sides of the membrane and 25, 50 and 75% of Na⁺ in the intracellular medium was replaced by TMA⁺ or TEA⁺. When Na⁺ ions were replaced by TMA⁺ differences among the CNGA1, CNGA1_{tandem} and CNGA1_{cys-free} channels were not statistically significant.

In contrast to what observed with TMA⁺ blockage, TEA⁺ blocked the cGMP activated current more potently in the CNGA1_{cys-free} channels than in CNGA1 and CNGA1_{tandem} channels. At positive voltages replacing the concentration of intracellular Na⁺ ions with TEA⁺ by 25, 50 and 75%, it decreased the cGMP current (see Fig. 2g). Differences between CNGA1 and CNGA1_{tandem} channels were not statistically significant, but the differences of CNGA1_{cys-free} with CNGA1 channels were important: in fact the significance was $**P < 0.01$ in all three cases. Also at negative voltages, i.e. at -100 mV the presence of 27.5, 55 and 82.5 mM TEA⁺ at the intracellular side of the membrane reduced the Na⁺ influx. Similarly to what observed at +100 mV differences between the CNGA1 and CNGA1_{tandem} channels were not statistically significant but differences with the CNGA1_{cys-free} channel were

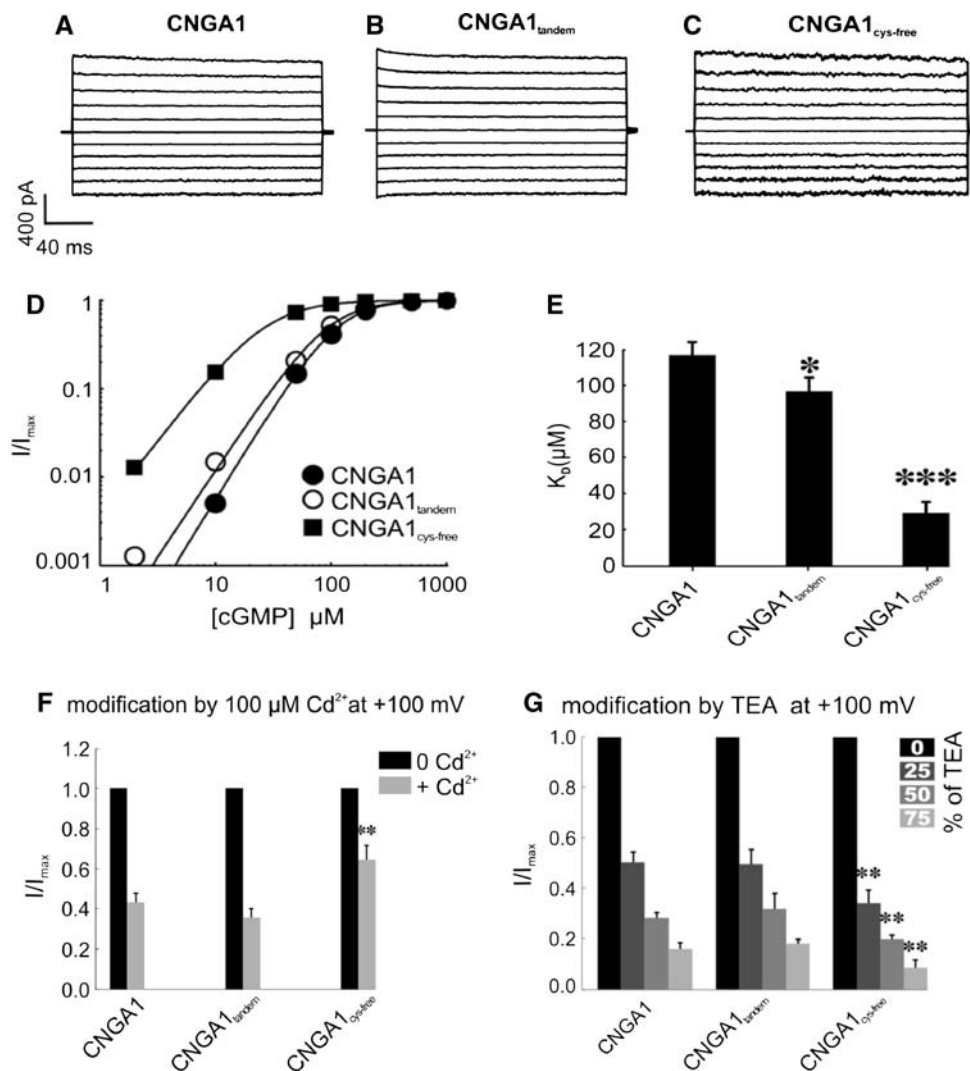


Fig. 2 Physiological differences between the three channels. **a**, **b** and **c** recordings of the cGMP activated current in voltage clamp experiments when the membrane voltage was stepped from -100 to $+100$ mV in 20 mV steps for the CNGA1, CNGA1_{tandem} and CNGA1_{cys-free} channels, respectively. Each trace was the average of five individual traces and the current was obtained as the difference between current recordings in the presence of 1 mM cGMP and current recordings obtained in the absence of cGMP. **d** The dose-response curve of cGMP activation at $+60$ mV for CNGA1 (closed circle), CNGA1_{tandem} (open circle) and CNGA1_{cys-free} (closed square) channels, respectively. The smooth curves are the fit to the equation $\frac{I}{I_{\max}} = \frac{[\text{cGMP}]^2}{[\text{cGMP}]^2 + [K_{1/2}]^2}$. Where I_{\max} is the maximum current elicited in the presence of 1 mM cGMP and $K_{1/2}$ is the concentration of the cGMP producing half maximal current. **e** Bar plot for the $K_{1/2}$ of the three channels. Statistical significance for differences of $K_{1/2}$ of CNGA1_{tandem} and CNGA1_{cys-free} to CNGA1 was checked by using Student's t test (see “Material and methods”). The difference in $K_{1/2}$ between CNGA1_{tandem} and CNGA1 channels has a marginal

significance ($*P < 0.05$). The difference of $K_{1/2}$ between CNGA1_{cys-free} and CNGA1 channels has very high significance ($***P < 0.0001$). **f** Comparison of Cd^{2+} blockage: bar plot showing the ratio of current measured at $+100$ mV in the presence of 1 mM cGMP with Cd^{2+} (+ Cd^{2+}) and the current measured with out Cd^{2+} (0 Cd^{2+}). Difference in Cd^{2+} blockage at $+100$ mV between CNGA1_{cys-free} and CNGA1 channels was significant ($**P < 0.001$), but CNGA1_{tandem} did not show an important difference compared to CNGA1 channels. **g** Blockage of Na^+ flux by TEA^+ ions: bar plot showing the modification of the Na^+ flux by TEA^+ at $+100$ mV. Bars are indicated in different grey levels indicating the percentage of TEA^+/Na^+ replacement: 0% indicates 110 mM NaCl, 25% is 87.5 mM NaCl + 22.5 mM TEACl, 50% is 55 mM NaCl + 55 mM TEACl and 75% is 27.5 mM NaCl + 87.5 mM TEACl. Blockage in CNGA1_{tandem} was not significantly different from that observed in CNGA1 channels. TEA^+ blockage in CNGA1_{cys-free} channels was statistically different from that observed in CNGA1 channels with a significance of $**P < 0.01$

significant with $*P < 0.05$ in the presence of 25% TEA^+ and $**P < 0.01$ in the presence of 50 and 75% of TEA^+ . TEA^+ effect was analyzed in the presence of a saturating cGMP concentration and therefore the different blockage

observed in the CNGA1 and CNGA1_{cys-free} channels cannot be ascribed to their different sensitivity to cGMP, as in the presence of 1 mM cGMP both channels have an open probability about 0.9 .

Electrophysiological similarities among the three channels

CNG channels differ from the other members of the superfamily of voltage gated channels (Jan and Jan 1990; Kaupp et al. 1989; Zagotta and Siegelbaum 1996) for their poor selectivity among monovalent alkali cations. The permeability ratio in the native CNG channels from rod photoreceptors (Menini 1990) is

$$\text{Li (1.14)} > \text{Na (1)} > \text{K (0.98)} > \text{Rb (0.84)} > \text{Cs (0.58)} \quad (1)$$

where the number in parenthesis indicates the selectivity ratio between the tested alkali monovalent cation and Na^+ . This permeability ratio differs from that of the homomeric CNGA1 channel (Kaupp et al. 1989; Nizzari et al. 1993):

$$\text{Na (1)} > \text{K (0.96)} > \text{Li (0.75)} > \text{Rb (0.73)} > \text{Cs (0.36)} \quad (2)$$

The presence of the CNGB1 subunit makes the native CNG channel more permeable to Li^+ than to Na^+ (Kaupp et al. 1989; Körschen et al. 1995). In this analysis, the selectivity to monovalent alkali cations was estimated by measuring V_{rev} in bi-ionic conditions, in saturating cGMP. The pipette always contained 110 mM NaCl, while the equimolar monovalent alkali cationic solutions were changed at the intracellular side of the patch. Currents were elicited by applying ± 40 mV in step of 2 mV across the patch membrane. A comparison of the measured V_{rev} among the three channels showed that the three channels had similar values of V_{rev} within the experimental variability.

It is well known that Ca^{2+} ions permeate through CNG channels but also block the current carried by Na^+ ions (Colamartino et al. 1991). Ca^{2+} ions block CNG channels from the extracellular side rather powerfully and the concentration of Ca^{2+} blocking half of the maximal current is voltage dependent and is 288 μM at +80 mV and 2.3 μM at −30 mV (Eismann et al. 1994). At the intracellular side Ca^{2+} ions block CNGA1 channels less powerfully and the Ca^{2+} concentration blocking half of the maximal cGMP activated current is 2.3 mM at +80 mV and 6.9 mM at −80 mV. Ca^{2+} blockage is partly mediated by Glu363 at the extracellular mouth of the inner pore (Root and MacKinnon 1993). In none of the three channels under investigation, Ca^{2+} ions potentiated the cGMP current at negative voltages, as observed in the presence of Cd^{2+} ions. Similar to Cd^{2+} ions, at positive voltages Ca^{2+} ions potentially blocked the cGMP activated current in a voltage dependent way. When data from all patches were considered for a statistical analysis, Ca^{2+} blockage in CNGA1_{cys-free}, CNGA1_{tandem} and in the WT CNGA1 channels was not significantly different.

Tetracaine at micromolar concentrations added to the intracellular side of the membrane blocks the CNGA1 channels (Fodor et al. 1997b) and is therefore a more potent blocker of CNGA1 channels than divalent cations, TMA^+ and TEA^+ . In the light of this, we have compared tetracaine blockage in the three channels under investigation. The blockage was measured at the end of voltage pulses lasting 100 ms. In the presence of 1 mM cGMP, the tetracaine concentration blocking half of the cGMP activated current $T_{1/2}$ at +80 mV was 5.3 ± 2.3 ($N = 6$), 4.2 ± 0.9 ($N = 5$) and 4.2 ± 0.9 ($N = 6$) μM for the CNGA1, CNGA1_{cys-free} and CNGA1_{tandem} channels, respectively. At −80 mV the values of $T_{1/2}$ was 11.77 ± 4.38 , 10.32 ± 4.31 and 8.88 ± 1.35 μM , respectively for the three channels. In agreement with a previous report (Fodor et al. 1997b) blockage by tetracaine in the presence of a lower cGMP concentration was stronger in all three channels. These results do not highlight any difference in tetracaine blockage in the three channels. Therefore ionic selectivity, Ca^{2+} and tetracaine blockage was very similar in the three channels.

Irreversible Cd^{2+} blockage in cysteine mutants in CNGA1 and CNGA1_{cys-free} channels

The comparison of physiological properties described in the previous sections has not identified any significant difference between the CNGA1 and CNGA1_{tandem} channels, but has indicated differences between the CNGA1 and CNGA1_{cys-free} channels. In the following session, we will attempt to quantify structural differences between these two channels.

The distance between residues in homologous subunits can be estimated by studying which cross-linking reagents, among those shown in Fig. 1, is able to cross-link the mutant channel obtained when these residues are mutated into cysteines. The existence of a residue cross-linked by reagents with different cross-linking span in the CNGA1 and CNGA1_{cys-free} channels provides a quantification of the structural difference between the two channels, at least for that residue. We have scanned the C-linker domain of CNGA1 channels looking for residues which when mutated in a cysteine in the CNGA1 channel background—but not in the CNGA1_{cys-free} channel background—lead to mutant channels blocked by Cd^{2+} ions. Several residues in this region were identified, such as Asn402, Ala406, Gln409, Asp413, Ala414, Gln417 and Tyr418. In order to find the appropriate residue we looked for a mutant channel where Cd^{2+} blockage was not altered when neighboring endogenous cysteines were replaced by residues not able to bind Cd^{2+} ions. With this rationale we identified Ala406 as the suitable residue. Therefore, we have studied the irreversible blockage of the cGMP activated current after a 5 min

application of 200 μM Cd^{2+} to the intracellular side of the membrane patch in the closed state in mutant channels A406C and A406C_{cys-free}. We use a concentration of 200 μM Cd^{2+} , which does not produce any significant change of the cGMP activated current in the WT CNGA1 channel and causes an irreversible blockage of the cGMP activated current in mutant channels N402C, A406C, Q409C, D413C, A414C and Q417C within 2 or 3 min.

As shown in Fig. 3a, the cGMP activated current observed in control conditions (left panel in Fig. 3a and b) was irreversibly blocked by Cd^{2+} ions in the mutant channel A406C (right panel of Fig. 3a), but not in the mutant channel A406C_{cys-free} (right panel of Fig. 3b). This different blocking effect of Cd^{2+} ions can be produced by two different mechanisms or by their combination. Cd^{2+} blockage of the cysteine mutant in the CNGA1 background illustrated in Fig. 3a can originate from Cd^{2+} coordination to the exogenous cysteine with endogenous cysteines and in particular with Cys481 and/or Cys505 (Mechanism 1) which are part of the C-linker domain (Brown et al. 1998).

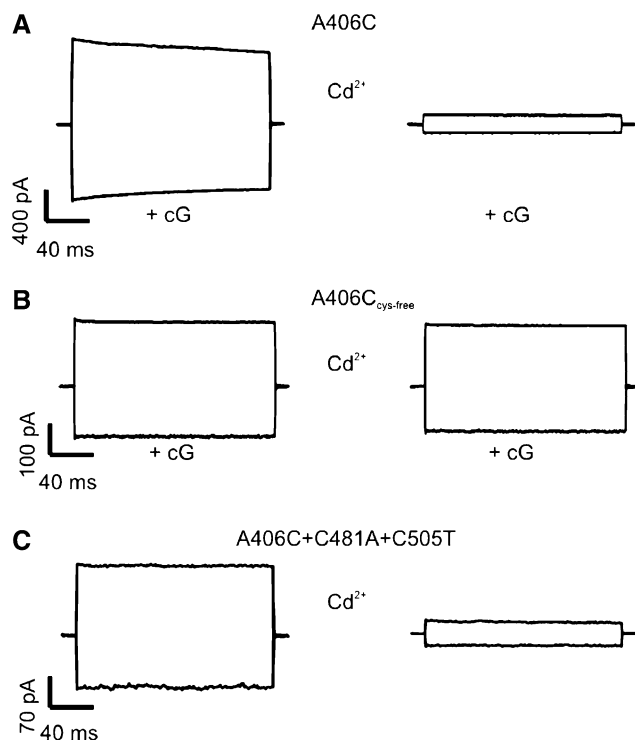


Fig. 3 In the closed state, Cd^{2+} blocks irreversibly A406C and A406C&C481A&C505T but not A406C_{cys-free}. The effect of 200 μM Cd^{2+} added for 5 min in mutant channel A406C (a), in mutant channel A406C_{cys-free} (b) and in mutant channel A406C&C481A&C505T (c). Cd^{2+} ions were added to the medium bathing the intracellular side of the membrane patch in the absence of cGMP. The left and right traces in a, b and c illustrate the current activated by 1 mM cGMP at ± 60 mV in control conditions and after exposure to Cd^{2+} ions, respectively. In the mutant channel A406C the irreversible blockage induced by 200 μM Cd^{2+} ions was $93 \pm 6\%$ ($N = 5$), and in the triple mutant it was $65 \pm 18\%$ ($N = 2$)

An alternative explanation is that the 3D structure of CNGA1_{cys-free} channels differs by some Å from CNGA1 channels (Mechanism 2), so that Cd^{2+} can coordinate exogenous cysteines introduced in the CNGA1 channels but not in the CNGA1_{cys-free} channels. In order to resolve this issue we studied in detail mutant channel A406C and we performed two series of experiments. In the first series of experiments we analysed Cd^{2+} blockage in cysteine mutant channels where the two endogenous cysteines Cys481 and Cys505 were replaced by residues not reacting with S atoms, such as alanine or threonine. In the second series of experiments the effect of cross-linkers of different length in mutant channel A406C_{cys-free} was examined.

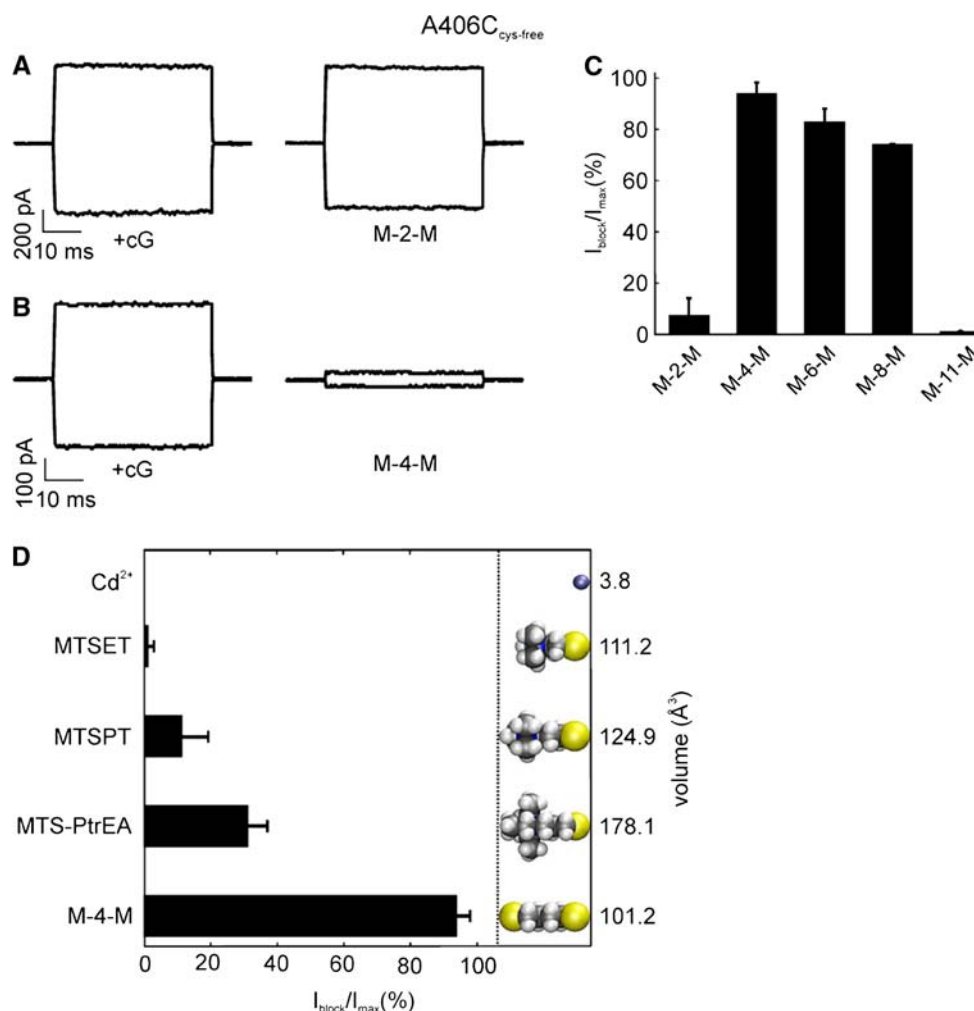
As shown in Fig. 3c Cd^{2+} blockage although slightly reduced is still observed in the triple mutant channel A406C&C481A&C505T. In the mutant channel A406C the irreversible blockage induced by 200 μM Cd^{2+} ions was $93 \pm 6\%$ ($N = 5$) and in the triple mutant it was $65 \pm 18\%$ ($N = 2$).

The effect of MTS cross-linkers on mutant channel A406C_{cys-free}

Cd^{2+} ions in the absence of cGMP powerfully blocked mutant channel A406C but not mutant channel A406C_{cys-free} (see Fig. 3a, b). The data presented in Fig. 3c indicate also that Cd^{2+} blockage in mutant channel A406C does not depend on the presence of endogenous cysteines at location 481 and 505 and therefore the observed Cd^{2+} blockage is primarily caused by its coordination to the ring of exogenously introduced cysteines at position 406. In this view, the absence of Cd^{2+} blockage observed in mutant channel A406C_{cys-free} is caused by a different 3D structure of the CNGA1 and CNGA1_{cys-free} channels, whereby in the CNGA1_{cys-free} channel residues at position 406 are at a different distance not allowing the coordination of Cd^{2+} ions by exogenous cysteines. In order to test this possibility, we investigated blockage by thiol cross-linkers M–X–M with an increasing length of the linker. A total of 100 μM of the cross-linker M–2–M did not block mutant channel 406C_{cys-free} ($N = 5$), as shown in Fig. 4a, c. In contrast, the same concentration of the reagent M–4–M ($N = 6$) powerfully blocked mutant channel A406C_{cys-free} (see Fig. 4b, c).

We have also analyzed blockage of the cGMP current in mutant A406C_{cys-free} by cross-linkers of increasing length. As shown in Fig. 4c, cross-linkers M–2–M ($N = 5$) and M–11–M ($N = 5$) did not block significantly mutant channel A406C_{cys-free}, while cross-linkers M–4–M ($N = 6$), M–6–M ($N = 4$) and M–8–M ($N = 6$) all blocked the mutant channel A406C_{cys-free}, with cross-linker M–4–M being the most potent blocker. M–2–M did not block the mutant channel A406C_{cys-free} probably because

Fig. 4 The sulfhydryl specific MTS cross-linkers block the A406C_{cys-free} channel. **a, b** represents the current traces in the control condition and after the application of cross-linkers. The current recordings shown are the response to ± 60 mV holding potential in the inside-out patch configuration. In **a** the first panel shows the control current from A406C_{cys-free} channels and the second after the application of M-2-M cross linker. In **b** as in **a** but after the application of M-4-M cross-linker. In A406C_{cys-free} 93.9 \pm 4.3% of the control current was blocked by M-4-M. **c** Bar plot showing the percent of blockage of the channel A406C_{cys-free} after the application of cross-linkers of varying length in the closed state. **d** Blockage of A406C_{cys-free} by different sulfhydryl reagents. On the right hand side of the panel the effective volumes of the reagents are shown with their 3D molecular structures



of its shorter cross-linking span. M-6-M and M-8-M cross-linkers exist in several rotamers (see Fig. 1) so that they can have an effective cross-linking span similar to that of M-4-M. We examined the effect of the M-2-M and M-4-M cross-linkers applied in the closed state of the mutant channels A406C and A406C&C481A&C505T. 100 μM M-2-M did not block either the mutant channel A406C ($10.4 \pm 9.4\%$; $N = 5$) or the triple mutant channel A406C&C481A&C505T ($12 \pm 10\%$; $N = 4$). Blockage by 100 μM M-4-M was also low with $13 \pm 9.7\%$ ($N = 5$) of the A406C channel and $5 \pm 4.5\%$ ($N = 4$) blockage of the triple mutant channel A406C&C481A&C505T.

The observed blockage of mutant channel 406C_{cys-free} by the cross-linker M-4-M could be caused by its binding to a single cysteine and a consequent steric blockage of the channel and not by its cross-linking to the two exogenous cysteines. A way to discriminate between these two mechanisms is to compare the effect of MTS compounds with an increasing volume. During the formation of an S-S bond, MTS compounds react and lose one SO_2CH_3 group. In this way the effective volume of MTS compounds

reacting with a cysteine decreases by about 30 \AA^3 . M-X-M cross linkers lose two SO_2CH_3 groups reducing their effective volume by about 60 \AA^3 (see Fig. 1). We then compared the blocking effect of 100 μM of different MTS compounds such as MTSET ($N = 6$), M-4-M ($N = 6$), MTSPT ($N = 4$) and MTSPtrEA ($N = 8$) (see Fig. 4d). MTSET is the shortest of the four compounds and MTSPtrEA is the bulkiest. As shown in Fig. 4d, MTSET is shorter than M-4-M; in contrast, MTSPT and MTSPtrEA have the same effective length of M-4-M but have a larger volume. If the mechanism of block caused by M-4-M is not mediated by cross-linking with two exogenous cysteines, also bulkier MTS compounds are expected to block the mutant channel A406C_{cys-free}. But as shown in Fig. 4d neither 100 μM MTSET ($N = 5$) nor the same concentration of MTSPT blocked the mutant A406C_{cys-free} ($N = 4$) and the same concentration of the much bulkier compound MTSPtrEA blocked $\sim 30\%$ ($N = 8$) of the current observed in the control condition (see Fig. 4d). These results show that the blockage observed by the M-4-M is caused by the cross-linking of exogenous cysteines. The

absence of Cd^{2+} blockage in mutant channel A406C_{cys-free} is ascribed to the fact that the 3D structure of the CNGA1 and CNGA1_{cys-free} is different and in particular residues at position 406 of the CNGA1_{cys-free} are at a reciprocal distance not compatible with Cd^{2+} coordination but compatible with the coordination by the cross-linker M–4–M. In the A406C mutant channel residues at position 406 are at a compatible reciprocal distance to coordinate with Cd^{2+} , but not with the longer cross-linkers M–2–M and M–4–M.

Discussion

Two constructs derived from the CNGA1 channels from bovine rods have been recently proposed as useful tools for the investigation of the relation between structure and function in CNGA1 channels. The first construct is the CNGA1_{cys-free} channels (Matulef et al. 1999), where all endogenous cysteines were replaced with other residues not bearing an S atom. The second construct is the CNGA1_{tandem} where two CNGA1 subunits are joined together by a small linker composed of some tens of residues (Flynn and Zagotta 2003; Liu and Siegelbaum 2000; Matulef and Zagotta 2002; Rosenbaum and Gordon 2002; Rothberg et al. 2002). However, it has not been proven that ionic channels formed by these constructs have a 3D structure identical or very similar to that of the CNGA1 channel. On the basis of their experimental investigation regarding the physiological properties of CNGA1 and CNGA1_{cys-free} channels, Matulef et al. (1999) concluded that mutation of all endogenous cysteines led to functional channels which were gated by cGMP in a way not too different from what observed in the CNGA1 channel. However, the degree of structural similarity between the CNGA1_{cys-free} and CNGA1 was not established. The investigation of electrophysiological properties of CNGA1, CNGA1_{tandem} and CNGA1_{cys-free} channels here presented, does not show any statistically significant difference between the CNGA1 and CNGA1_{tandem} channels. Several electrophysiological properties are remarkably similar and almost identical in CNGA1 and CNGA1_{cys-free} channels, but these two channels differ in a significant way for their sensitivity to cGMP, Ca^{2+} ions TEA^+ .

Functional differences between native and cysteine free proteins have already been reported and investigated. Significant differences were observed in the B Glutathione Synthetase from *Escherichia coli* (Kato et al. 1988), the P-glycoprotein (Taylor et al. 2001) and the rat renal Na^+/P_i cotransporter (Kohler et al. 2003), but their structural differences was not quantified. Results obtained with different MTS cross-linkers and reagents suggest that the

distance between homologous residues at position 406 in CNGA1_{cys-free} is longer than in the CNGA1 by 3–4 Å.

Electrophysiological differences between the CNGA1 and CNGA1_{tandem} channels

The I/V relations, ionic selectivity, dose response of the cGMP activated current and blockage by Ca^{2+} and Cd^{2+} ions, tetracaine, TMA^+ and TEA^+ in CNGA1_{tandem} and CNGA1 channels are not different. Since there is no electrophysiological difference between these two channels, we can then deduct that their 3D structure is very similar even though we cannot provide a precise estimate of this similarity.

Electrophysiological differences between the CNGA1 and CNGA1_{cys-free} channels

The I/V relations, ionic selectivity, blockage by Ca^{2+} ions, tetracaine and TMA^+ in CNGA1_{cys-free} and CNGA1 channels are not different. However, three quantitative differences were observed in the electrophysiological properties of the CNGA1 and CNGA1_{cys-free} channels. First, as shown in Fig. 2 the concentration of cGMP activating half of the maximal current $K_{1/2}$ was 116.9 ± 7.2 and 27.5 ± 6.1 for the CNGA1 and CNGA1_{cys-free} channels, respectively, in agreement with what already observed by Matulef et al. (1999). Second, as shown in Fig. 2, at +100 mV, a concentration of 100 μM Cd^{2+} ions added to the intracellular side of the membrane blocked CNGA1_{cys-free} to a lower extent than CNGA1 channels. Third, as shown in Fig. 2 and discussed in the text when Na^+ ions were replaced with TEA^+ , the cGMP activated current at both +100 and –100 mV decreased more in CNGA1_{cys-free} than in CNGA1 channels. These differences were statistically significant. Blockage by Ca^{2+} ions and by the organic compound TMA^+ was not significantly different in CNGA1 and CNGA1_{cys-free} channels.

Structural differences between the CNGA1 and CNGA1_{cys-free} channels

The remarkable similarity of several functional properties between the CNGA1_{cys-free} and the CNGA1 channels indicates that the 3D structure of the CNGA1 channels does not depend critically on the presence of cysteines and suggests that S–S bridges neither determine the 3D structure of a monomer nor their coassembly in a functional tetrameric channel. The similarity of ionic selectivity and blockage by Ca^{2+} ions, TMA^+ and tetracaine indicates that the 3D structure of the two channels in the pore region is very similar but not identical: indeed Cd^{2+} and TEA^+ blockage is different. The blockage of an ionic channel can

be modulated by the position and properties of a single residue (Bucossi et al. 1996; Gordon and Zagotta 1995) and significant functional differences can originate from very small structural changes often of the order of just 1 Å or less. For instance, single channel properties of the CNGA1 channel change when the length of the side chain at position 363 is reduced by 1 Å in the mutant E363D (Bucossi et al. 1997).

As sensitivity to cGMP depends on structural changes initiated by its binding in the CNB domain leading to modifications in the pore region, it is not surprising that the dose response in CNGA1 and CNGA1_{cys-free} to be different: indeed the dose response is expected to be sensitive to the global 3D structure of the channel. In order to quantify differences in the 3D structure of CNGA1 and CNGA1_{cys-free} channels, we looked for a residue of the CNGA1 channel, which, when mutated into a cysteine, could cross-link with another cysteine at the same position but from a different subunit. The length of the cross-linker is a good indicator of the distance between homologous residues in different subunits: if Cd²⁺ ion is the cross-linking reagent, the distance between the C_α of the homologous residues is between 8 and 11 Å. The reagents M–2–M, M–4–M and M–6–M are molecules with an S atom at both ends separated by a handle of variable lengths (Loo and Clarke 2001). If the same residue in the CNGA1_{cys-free} channel is not cross-linked by a Cd²⁺ ion but by an M–X–M reagent, the length of the handle provides an estimate of the different distance between homologous residues in the CNGA1 and CNGA1_{cys-free} channels. As discussed at the beginning of “Results”, endogenous cysteines possibly contributing to Cd²⁺ binding in mutant channel A406C are Cys481 and Cys505. As shown in Fig. 3 in the absence of cGMP, Cd²⁺ ions powerfully and irreversibly block mutant channel A406C and the triple mutant channel A406C&C481A&C505T. These results indicate that the observed irreversible Cd²⁺ blockage in mutant channel A406C can be ascribed to a cross-linking reaction between exogenous cysteines in homologous positions. By contrast, the mutant channel A406C_{cys-free} in the absence of cGMP is not blocked by Cd²⁺ ions but is blocked by 100 μM of the cross-linker M–4–M (see Fig. 4). Mutant channel A406C_{cys-free} is not blocked by 100 μM MTSET, which has a slightly higher volume than M–4–M. Furthermore, two other MTS derivatives MTSP (Sullivan and Cohen 2000) and MTS-PtrEA (Contreras and Holmgren 2006) with same length as M–4–M but with much higher volume did not block the channel. Therefore, blockage of the mutant channel A406C_{cys-free} in the absence of cGMP by M–4–M is ascribed to the cross-linkage of exogenous cysteines in two subunits. These results are summarized in Fig. 5.

The C_α of residues at position 406 of the CNGA1 are at distance of about 8–11 Å, but the distance between the same residues in the CNGA1_{cys-free} channel is longer by several Angstrom, so that one Cd²⁺ cross-links homologous residues in the CNGA1 channel but not in the CNGA1_{cys-free} channel. In the CNGA1_{cys-free} channel the reagent M–4–M is necessary to cross-link the same homologous residues, so that the distance between their C_α is about 14.5 Å, i.e. approximately 3 Å more than in the CNGA1 channel. As the strength and nature of chemical interactions change drastically when distances are increased by 3–4 Å, the way in which the CNGA1 and CNGA1_{cys-free} channels interact with chemical probes can be completely different. This conclusion is not surprising, as when all cysteines are removed from a protein the overall 3D structure can change quite significantly. Indeed we have previously shown that it was possible to lock the mutant channel F380C channel in the open and closed state, but *only to some extent* when Phe380 is replaced with a cysteine in the CNGA1_{cys-free} channel (Nair et al. 2006).

It is concluded that physiological properties of the CNGA1 and CNGA1_{cys-free} are remarkably similar, despite the major role of cysteines in the determination of protein structure. However, the 3D structure of these two channels is not identical and indeed distances between homologous residues can be different by some Å.

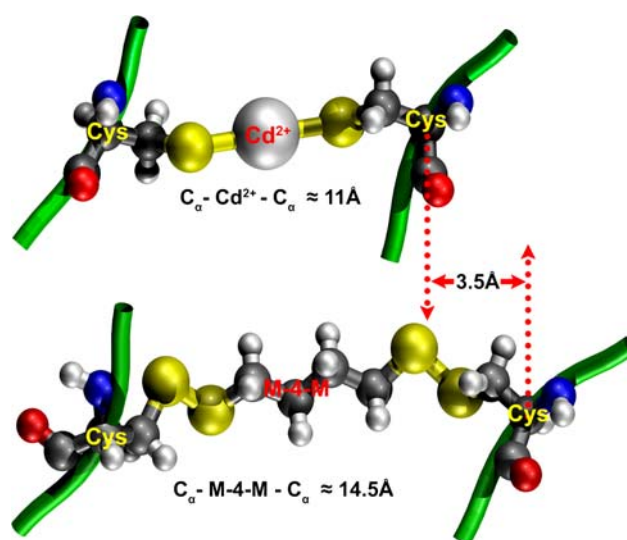


Fig. 5 The distance between homologous residues at position 406 in the CNGA1 and CNGA1_{cys-free} channels. A model of the binding of Cd²⁺ and M–4–M to CNGA1 and CNGA1_{cys-free} channels, respectively. The green tube represents part of S6 helix where the mutated A406C is positioned. The sulfur atom of cysteine is shown as yellow spheres, coordinating with a Cd²⁺ in the CNGA1 channel and cross-links with the sulfur atoms from both ends of M–4–M in the CNGA1_{cys-free} channel. The difference in the distance between the C_α of the two channels is about 3.5 Å

Acknowledgments We are extremely thankful to William Zagotta who very generously supplied us with the clone of the CNGA1 and CNGA1_{cys-free} channels and Claudio Anselmi for helpful discussions. This work was supported by a HFSP grant, a COFIN grant from the Italian Ministry, a grant from CIPE (GRAND FVG) and a FIRB grant from MIUR.

References

- Akabas MH, Stauffer DA, Xu M, Karlin A (1992) Acetylcholine receptor channel structure probed in cysteine-substitution mutants. *Science* 258:307–310
- Becchetti A, Gamel K (1999) The properties of cysteine mutants in the pore region of cyclic-nucleotide-gated channels. *Pflügers Arch* 438:587–596
- Becchetti A, Gamel K, Torre V (1999) Cyclic nucleotide-gated channels pore topology studied through the accessibility of reporter cysteines. *J Gen Physiol* 114:377–392
- Biel M, Zong X, Ludwig FA, Sautter A, Hofmann F (1999) Structure and function of cyclic nucleotide-gated channels. *Rev Physiol Biochem Pharmacol* 135:151–171
- Bradley J, Frings S, Yau KW, Reed R (2001) Nomenclature for ion channel subunits. *Science* 294:2095–2096
- Brown RL, Snow SD, Haley TL (1998) Movement of gating machinery during activation of rod cyclic nucleotide-gated channels. *Biophys J* 75:825–833
- Bucossi G, Eismann E, Sesti F, Nizzari M, Seri M, Kaupp UB, Torre V (1996) Time-dependent current decline in cyclic GMP-gated bovine channels caused by point mutations in the pore region expressed in *Xenopus* oocytes. *J Physiol (Lond)* 493:409–418
- Bucossi G, Nizzari M, Torre V (1997) Single-channel properties of ionic channels gated by cyclic nucleotides. *Biophys J* 72:1165–1181
- Colamartino G, Menini A, Torre V (1991) Blockage and permeation of divalent cations through the cyclic GMP-activated channel from tiger salamander retinal rods. *J Physiol* 440:189–206
- Contreras JE, Holmgren M (2006) Access of quaternary ammonium blockers to the internal pore of cyclic nucleotide-gated channels: implications for the location of the gate. *J Gen Physiol* 127:481–494
- Craven KB, Zagotta WN (2006) CNG and HCN channels: two peas, one pod. *Annu Rev Physiol* 68:375–401
- Eismann E, Muller F, Heinemann SH, Kaupp UB (1994) A single negative charge within the pore region of a cGMP-gated channel controls rectification, Ca²⁺ blockage, and ionic selectivity. *Proc Natl Acad Sci USA* 91:1109–1113
- Fesenko EE, Kolesnikov SS, Lyubarsky AL (1985) Induction by cyclic GMP of cationic conductance in plasma membrane of retinal rod outer segment. *Nature* 313:310–313
- Flynn GE, Zagotta WN (2003) A cysteine scan of the inner vestibule of cyclic nucleotide gated channels reveals architecture and rearrangement of the pore. *J Gen Physiol* 121:563–582
- Fodor AA, Black KD, Zagotta WN (1997a) Tetracaine reports a conformational change in the pore of cyclic nucleotide-gated channels. *J Gen Physiol* 110:591–600
- Fodor AA, Gordon SE, Zagotta WN (1997b) Mechanism of tetracaine block of cyclic nucleotide-gated channels. *J Gen Physiol* 109:3–14
- Glusker JP (1991) Structural aspects of metal liganding to functional groups in proteins. *Adv Protein Chem* 42:1–76
- Gordon SE, Varnum MD, Zagotta WN (1997) Direct interaction between amino- and carboxyl-terminal domains of cyclic nucleotide-gated channels. *Neuron* 19:431–441
- Gordon SE, Zagotta WN (1995) Subunit interactions in coordination of Ni²⁺ in cyclic nucleotide-gated channels. *Proc Natl Acad Sci USA* 92:10222–10226
- Hastrup H, Karlin A, Javitch JA (2001) Symmetrical dimer of the human dopamine transporter revealed by cross-linking Cys-306 at the extracellular end of the sixth transmembrane segment. *Proc Natl Acad Sci USA* 98:10055–10060
- Humphrey W, Dalke A, Schulten K (1996) VMD: visual molecular dynamics. *J Mol Graph* 14:33–38
- Jan LY, Jan YN (1990) A superfamily of ion channels. *Nature* 345:672
- Karlin A, Akabas MH (1998) Substituted-cysteine accessibility method. In: Conn PM (Ed) *Methods in enzymology*. Academic Press, San Diego pp. 123–145
- Kato H, Tanaka T, Nishioka T, Kimura A, Oda J (1988) Role of cysteine residues in glutathione synthetase from *Escherichia coli* B. Chemical modification and oligonucleotide site-directed mutagenesis. *J Biol Chem* 263:11646–11651
- Kaupp UB, Niidome T, Tanabe T, Terada S, W.Bönigk, W.Stühmer, Cook NJ, Kangawa K, Matsuo H, Hirose T, Miyata T, Numa S (1989) Primary structure and functional expression from complementary DNA of the rod photoreceptor cyclic GMP-gated channel. *Nature* 342:762–766
- Kaupp UB, Seifert R (2002) Cyclic nucleotide gated channels. *Physiol Rev* 82:769–824
- Köhler K, Förster IC, Stange G, Biber J, Murer H (2003) Essential cysteine residues of the type IIa Na⁺/Pi cotransporter. *Pflügers Arch* 446:203–210
- Körtschen HG, Illing M, Seifert R, Sesti F, Williams A, Gotzes S, Colville C, Müller F, Dosé A, Godde M (1995) A 240 kDa protein represents the complete beta subunit of the cyclic nucleotide-gated channel from rod photoreceptor. *Neuron* 15:627–636
- Liu J, Siegelbaum SA (2000) Change of pore helix conformational state upon opening of cyclic nucleotide gated channels. *Neuron* 28:899–909
- Loo TW, Clarke DM (2001) Determining the dimensions of the drug-binding domain of human P-glycoprotein using thiol cross-linking compounds as molecular rulers. *J Biol Chem* 276:36877–36880
- Matulef K, Flynn GE, Zagotta WN (1999) Molecular rearrangements in the ligand-binding domain of cyclic nucleotide-gated channels. *Neuron* 24:443–452
- Matulef K, Zagotta W (2002) Multimerization of the ligand binding domains of cyclic nucleotide-gated channels. *Neuron* 36:93–103
- Matulef K, Zagotta WN (2003) Cyclic nucleotide-gated ion channels. *Annu Rev Cell Dev Biol* 19:23–44
- Menini A (1990) Currents carried by monovalent cations through cyclic GMP-activated channels in excised patches from salamander rods. *J Physiol* 424:167–185
- Molday RS, Molday LL, Dose A, I.Clark-Lewis, Illing M, Cook NJ, Eismann E, Kaupp UB (1991) The cGMP-gated channel of the rod photoreceptor cell characterization and orientation of the amino terminus. *J Biol Chem* 266:21917–21922
- Nair AV, Mazzolini M, Codega P, Giorgetti A, Torre V (2006) Locking CNGA1 channels in the open and closed state. *Biophys J* 90:3599–3607
- Nizzari M, Sesti F, Giraudo MT, Virginio C, Cattaneo A, Torre V (1993) Single-channel properties of cloned cGMP-activated channels from retinal rods. *Proc R Soc Lond* 254:69–74
- Picco C, Menini A (1993) The permeability of the cGMP-activated channel to organic cations in retinal rods of the tiger salamander. *J Physiol* 460:741–758
- Ren X, Nicoll DA, Philipson KD (2006) Helix packing of the cardiac Na⁺–Ca²⁺ exchanger: proximity of transmembrane segments 1, 2, and 6. *J Biol Chem* 281:22808–22814
- Root MJ, MacKinnon R (1993) Identification of an external divalent binding site in the pore of a cGMP-activated channel. *Neuron* 11:459–466

- Rosenbaum T, Gordon SE (2002) Dissecting intersubunit contacts in cyclic nucleotide-gated ion channels. *Neuron* 33:703–713
- Rothberg B, Shin K, Phale P, Yellen G (2002) Voltage-controlled gating at the intracellular entrance to a hyperpolarization-activated cation channel. *J Gen Physiol* 119:83–91
- Sesti F, Eismann E, Kaupp UB, Nizzari M, Torre V (1995) The multi-ion nature of the cGMP-gated channel from vertebrate rods. *J Physiol (Lond)* 487:17–36
- Shapiro SS, Wilk MB (1965) An analysis of variance test for normality (complete samples). *Biometrika* 52:591–611
- Snedecor GW, Cochran WG (1989) Statistical methods, 8th edn. Blackwell, Oxford, pp 98–99
- Sullivan DA, Cohen JB (2000) Mapping the agonist binding site of the nicotinic acetylcholine receptor. Orientation requirements for activation by covalent agonist. *J Biol Chem* 275:12651–12660
- Sun ZP, Akabas MH, Goulding EH, Karlin A, Siegelbaum SA (1996) Exposure of residues in the cyclic nucleotide-gated channel pore: P region structure and function in gating. *Neuron* 16:141–149
- Taylor AM, Storm J, Soceneantu L, Linton KJ, Gabriel M, Martin C, Woodhouse J, Blott E, Higgins CF, Callaghan R (2001) Detailed characterization of cysteine-less P-glycoprotein reveals subtle pharmacological differences in function from wild-type protein. *Br J Pharmacol* 134:1609–1618
- Varnum MD, Zagotta WN (1996) Subunit interactions in the activation of cyclic nucleotide-gated ion channels. *Biophys J* 70:2667–2679
- Weitz D, Ficek N, Kremmer E, Bauer PJ, Kaupp UB (2002) Subunit stoichiometry of the CNG channel of rod photoreceptors. *Neuron* 36:881–889
- White D, Taverner CB, Leach PGL, Coville NJ (1993) Quantification of substituent and ligand size by the use of solid angles. *J Comp Chem* 14:1042–1049
- Zagotta WN, Siegelbaum SA (1996) Structure and function of cyclic nucleotide-gated channels. *Annu Rev Neurosci* 19:235–263
- Zheng J, Trudeau MC, Zagotta WN (2002) Rod cyclic nucleotide-gated channels have a stoichiometry of three CNGB1 subunits and one CNGB1 subunit. *Neuron* 36:891–896
- Zhong H, Molday LL, Molday RS, Yau KW (2002) The heteromeric cyclic nucleotide-gated channel adopts a 3A:1B stoichiometry. *Nature* 420:193–198